

Time Domain Analysis of Ultra-Wide Band Signals from Buried Objects Under Flat and Slightly Rough Surfaces

S. MakalYucedag and A. Kizilay

Department of Electronics and Communications Engineering
Yildiz Technical University, Istanbul, 34349, Turkey
smakal@yildiz.edu.tr and akizilay@yildiz.edu.tr

Abstract — The analysis of transient scattering for TM_z (horizontally) polarization from a cylindrical perfectly conducting (PEC) object buried in a lossy medium is considered. Flat and slightly surface cases are considered for the dielectric half-space. Our previous work using a decomposition method solution in frequency domain of TM_z polarization is utilized to solve this scattering problem. Then, an inverse Fourier transform is used to get the time domain signals. Timing analysis is done by calculating the travelling time of reflected signals in the possible paths. Then, multiple reflections are identified using these travelling times. Finally, the results from the flat and slightly rough surface profiles are used to compare the effects of multipath propagation.

Index Terms - Buried object, electromagnetic scattering, and multipath analysis.

I. INTRODUCTION

There exists much interest in ground penetrating radar (GPR). Therefore, significant attention has been directed toward the study of scattering from buried targets and several techniques have been employed to calculate the scattered fields [1-5]. Then, these results are used to obtain information for buried objects and design new GPR systems [6-13].

Recently, the applications of GPR using ultra-wideband (UWB) short-pulse radars attract more interest than the ones using narrow-band radars [14-22]. This is because the field scattered by targets illuminated by an UWB short pulse contains information such as location, strength of diffracting centers, dispersive phenomena and

resonances [23]. Also, if buried targets are interrogated by an UWB short pulse, clutter and multipath interference in received signal are reduced [24]. In order to examine the scattering of UWB short-pulse radars signal from buried targets, UWB short-pulse plane-wave scattering from buried PEC object is considered in this study. Also, to understand the effect of the surface roughness on UWB scattering, flat, and slightly rough surface profiles are used.

Consider a TM_z plane wave with the incident angle ϕ_i and it is assumed to be incident on a cylindrical object of arbitrary cross-section buried in a two-dimensional infinite surface as shown in

Fig. 1. A PEC object is located h_c below the x -axis. The distance between the y -axis and the object axis is indicated by x_c , the height and width of one period of the rough surface are represented by h_p and w_p , respectively.

Previously, a decomposition solution method has been obtained for the electromagnetic field scattered by a PEC cylindrical object with an arbitrary cross-section buried in a lossy dielectric half space with flat surface in [25] and periodic surface in [26]. Using this solution method, the scattered electric field is obtained in an ultra-wide frequency band, and then the time-domain scattered fields are synthesized via inverse Fourier transform. Finally, these scattering results are used to investigate the effects of multipath.

II. MULTIPATH ANALYSIS

To analyze the multiple reflections from a PEC cylindrical object buried in a sinusoidal surface, initially the scattering from a cylinder under a flat surface is considered. Gathering the basic knowledge of the multipath phenomenon

from the flat surface model, the analysis extended to a sinusoidal periodic surface case.

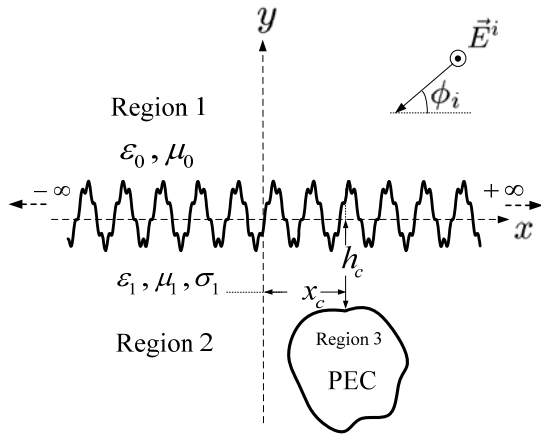


Fig. 1. Geometry of cylindrical object buried inside a lossy half-space with periodic surface.

The geometries and parameters of the buried PEC cylinder in medium with flat and sinusoidal surface indicated in Fig. 2 (a) and (b) are used for time domain results. As seen in these figures, the object is chosen to be a PEC cylinder with circular cross-section of radius r_a . The surface represents by,

$$y(x) = h_p \cos(2\pi x/w_p). \quad (1)$$

The transient signal scattered by a buried PEC cylinder's temporal characteristics can be identified easily using ray tracing. For the normal incidence ($\phi_i = 90^\circ$), the first two reflections from a cylinder under an infinite flat surface are shown in

Fig. 3. The first one is coming from the cylinder (L_1) and the second one is coming from the flat surface-cylinder-flat surface path (L_2). The time passing between these two reflections is calculated by

$$\Delta t_{1c} = \frac{(L_2 - L_1)\sqrt{\epsilon_{r1}}}{c}, \quad (2)$$

where ϵ_{r1} is the relative permittivity of the medium and c is the speed of light in space [20]. It is expected to have more reflections because of multiple bounce of the signal between the surface and the target. Other reflection's travelling paths are going to be multiples of L_1 . Therefore, the time past between two successive reflections can be calculated by a generalized form of equation (2),

$$\Delta t_c = \frac{L_1\sqrt{\epsilon_{r1}}}{c}. \quad (3)$$

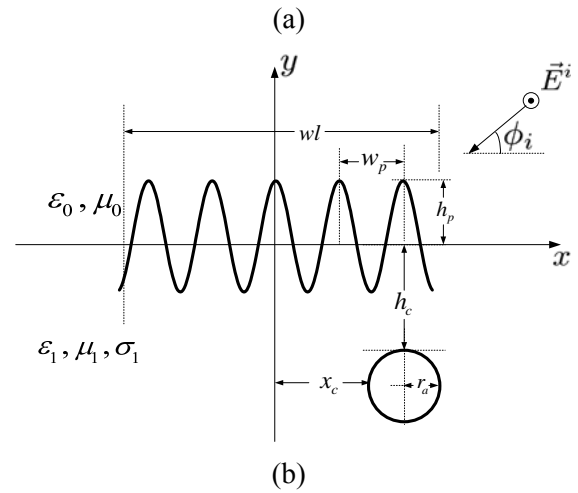
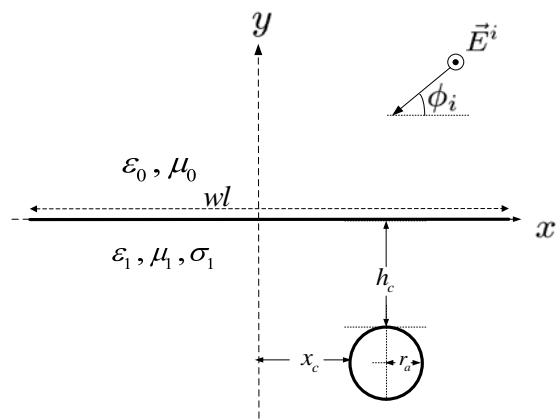


Fig. 2. The medium with (a) flat surface and (b) sinusoidal surface.

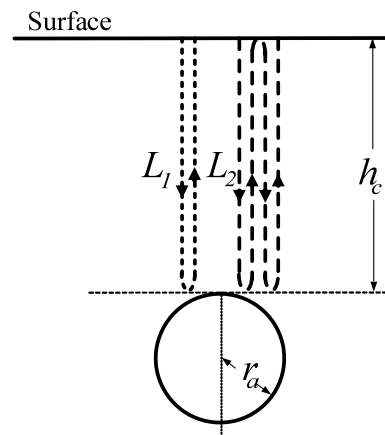


Fig. 3. Expected reflections from a buried cylindrical object.

III. TIME DOMAIN RESULTS

The incident signal is constructed from a frequency spectrum of 1-30 GHz with 726 data points. This frequency data is weighted using a double Gaussian function,

$$W_{dg}(f) = \sqrt{\frac{\pi}{\alpha_1}} a_1 \exp\left(-\frac{(\pi f)^2}{\alpha_1}\right) - \sqrt{\frac{\pi}{\alpha_2}} a_2 \exp\left(-\frac{(\pi f)^2}{\alpha_2}\right) \quad (4)$$

$$\alpha_1 = \frac{\pi}{\tau_1^2}, \quad \alpha_2 = \frac{\pi}{\tau_2^2}, \quad (5)$$

$$a_1 = \frac{\sqrt{\alpha_1}}{\sqrt{\alpha_1} - \sqrt{\alpha_2}}, \quad a_2 = \frac{\sqrt{\alpha_2}}{\sqrt{\alpha_1} - \sqrt{\alpha_2}}, \quad (6)$$

with the values of $\tau_1 = 0.04 \times 10^{-9}$ and $\tau_2 = 0.0625 \times 10^{-9}$ and shown in

Fig. 4 (a). Then, the weighted frequency data is transformed into time domain using an inverse Fourier transform. The resulting transient incident TM_z signal is shown in

Fig. 4 (b). The backscattered field from a PEC cylinder in free space is shown in both the frequency and time domains in Fig. 5. As expected the reflected field has a sign change because of a single reflection from a PEC surface seen in time domain result in Fig. 5 (b).

The backscattered field from a buried PEC cylinder is shown in time domain in Fig. 6. In Fig. 6, $L_1 = 2h_c$, $L_2 = 2L_1$, and ϵ_{r1} is chosen as 15. In TableI, the time past between two signals calculated by using equation (3) and the time found from the figure are indicated by Δt_c and Δt_r , respectively. In the figures, ϕ_s is the scattering angle. To investigate the effect of the burial depth of the cylinder, it is located nearer to the surface than the one in Fig. 6. Then, the backscattered field is calculated and shown in time domain in Fig. 7. It is observed that the time between the reflections decreases. There are four main reflections following the paths L_1 , L_2 , L_3 , and L_4 . Here, $L_1 = 2h_c$, $L_2 = 2L_1$, $L_3 = 3L_1$, $L_4 = 4L_1$, and TableII shows the comparison of timings.

The effect of the medium loss to the time domain signal is shown in Fig. 8. As expected, as the loss of the medium increases, the amplitude of the scattered field decreases. To investigate effect of the incidence angle on the scattered field, the incident angle is chosen as $\phi_i = 20^\circ$. Then, the backscattered field is calculated and shown in time domain in Fig. 9. The time between the successive reflections can be calculated by,

$$\Delta t'_c = \frac{L_1 \sqrt{\epsilon_{r1}}}{\sin(\phi_i) c} \quad (7)$$

where ϕ_i is the angle measured from normal of the surface and found as $\phi_i = 14^\circ$. The comparison of timings is given in

TableIII.

The backscattered field from a PEC cylinder under a slightly rough surface is shown in Fig. 10 to 13. In Fig. 10, the expected paths are L_1 , L_2 , L_3 , L_4 , L_5 . For the slightly rough surface case, the roughness should be included in the timing analysis so $L_j = h_c + h_p$ and the lengths of other paths are multiples of L_1 . The signals are assumed to travel the same paths as the signals in the flat surface case. The comparisons of timings for Fig. 10 are given in TableIV. The results are very close to flat surface results. To investigate the effect of the depth of the object, the object is buried deeper and the result is shown in Fig. 11. The expected paths are L_1 , L_2 , and L_3 . The comparisons of timings for Fig. 11 are given in TableV. As it is expected the number of signals is reduced because the signals travel greater distances and as a result attenuate more. However, the results are still very close to flat surface results.

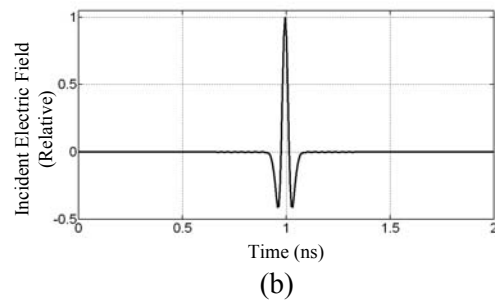
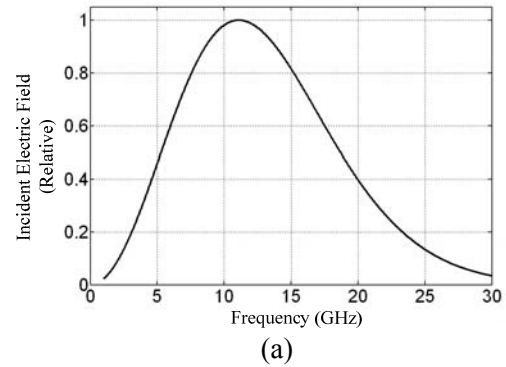


Fig. 4. The incident E-field waveform (a) in frequency and (b) time domains.

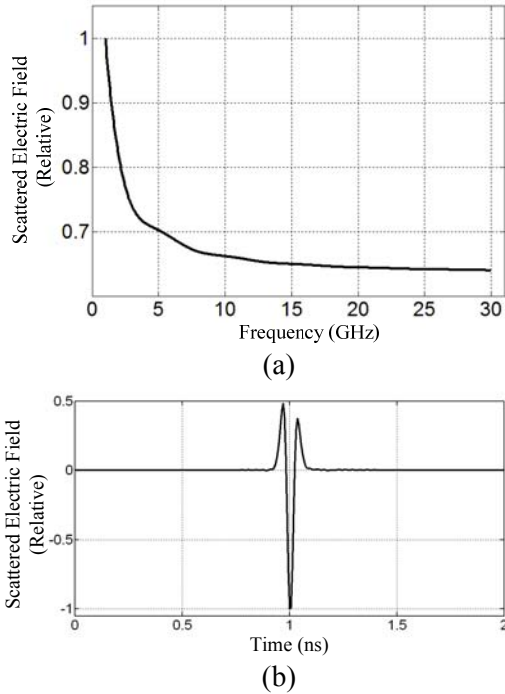


Fig. 5. TM_z backscattered field from a cylindrical PEC object with $r_a = 0.01$ m (a) at frequency and (b) time domains.

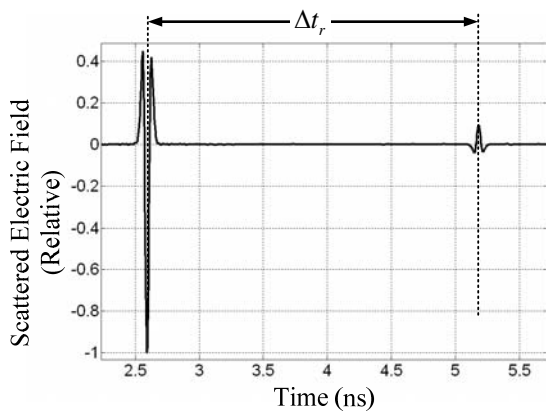


Fig. 6. TM_z backscattered field from a buried cylindrical PEC object for $r_a = 0.01$ m, $h_c = 0.1$ m, $wl = 2$ m, $x_c / r_a = 0.0$, $\epsilon_1 = 15 \epsilon_0$ F/m, $\mu_1 = \mu_0$ H/m, $\phi_i = \phi_s = 90^\circ$, and $\sigma_1 = 0.001$ Sm^{-1} .

Table I: Comparison of timings for the case shown in Fig. 6.

Δt_c (ns)	Δt_r (ns)
2.582	2.594

The depth of the object is increased and results are shown in Fig. 12 and 13, for $\phi_i = \phi_s = 90^\circ$ and $\phi_i = \phi_s = 20^\circ$, respectively. But the results are very complicated compare to the flat surface results. It is observed that the surface roughness started to affect the scattered field greatly because the incident wave can find more paths to reflect from the object. The relative time Δt_r between this two groups are found from Fig. 12 and 13 as 2.6260 ns and 2.8420 ns, respectively. These time values are similar to the case of flat surface found from Fig. 6 and 9. Thus, the beginning of the first group and the last group of reflections are following the paths of L_1 and L_2 , respectively. These groups of reflections contain some reflections caused by the surface roughness. However, their paths are difficult to identify.

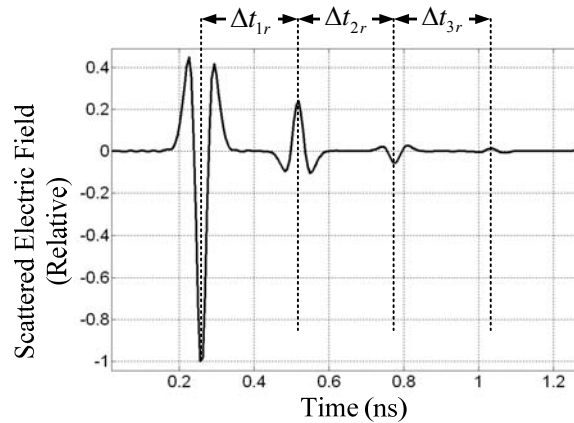


Fig. 7. TM_z back scattered field from a buried cylindrical PEC object for $r_a = 0.01$ m, $h_c = 0.01$ m, $wl = 2$ m, $x_c / r_a = 0.0$, $\epsilon_1 = 15 \epsilon_0$ F/m, $\mu_1 = \mu_0$ H/m, $\phi_i = \phi_s = 90^\circ$, and $\sigma_1 = 0.001$ Sm^{-1} .

Table II: Comparison of timings for the case shown in Fig. 7.

n	Δt_c (ns)	Δt_{nr} (ns)
1	0.2582	0.2625
2	0.2582	0.2564

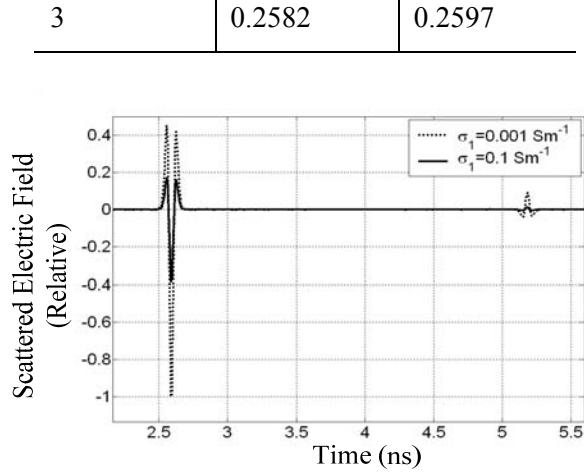


Fig. 8. TM_z back scattered field from a buried cylindrical PEC object for $r_a = 0.01$ m, $h_c = 0.1$ m, $wl = 2$ m, $x_c / r_a = 0.0$, $\epsilon_1 = 15 \epsilon_0$ F/m, $\mu_1 = \mu_0$ H/m, and $\phi_i = \phi_s = 90^\circ$.

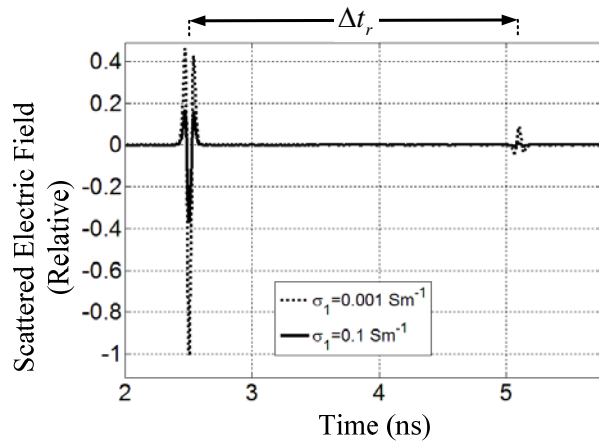


Fig. 9. TM_z back scattered field from a buried cylindrical PEC object for $r_a = 0.01$ m, $h_c = 0.1$ m, $wl = 2$ m, $x_c / r_a = 0.0$, $\epsilon_1 = 15 \epsilon_0$ F/m, $\mu_1 = \mu_0$ H/m, $\phi_i = \phi_s = 20^\circ$, and $\sigma_1 = 0.001 \text{ Sm}^{-1}$.

Table III: Comparison of the timings for the case shown in Fig. 9.

$\Delta t'_c$ (ns)	Δt_r (ns)
2.661	2.594

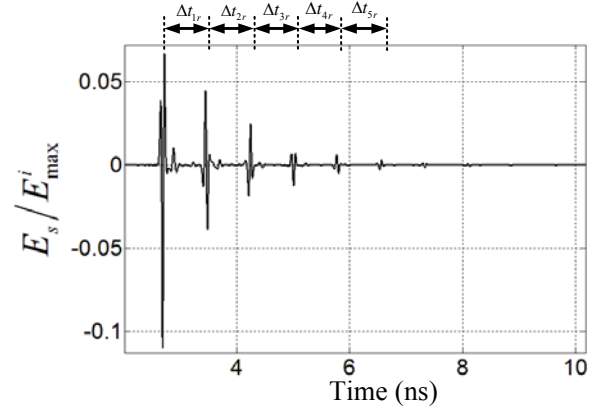


Fig. 10. TM_z back scattered field from a buried cylindrical PEC object for $r_a = 0.01$ m, $h_c = 0.02$ m, $wl = 2$ m, $x_c / r_a = 0.0$, $\epsilon_1 = 15 \epsilon_0$ F/m, $\mu_1 = \mu_0$ H/m, $\phi_i = \phi_s = 90^\circ$, $w_p = 0.1$ m, $h_p / w_p = 0.1$, and $\sigma_1 = 0.001 \text{ Sm}^{-1}$.

Table IV: Comparison of timings for the case in Fig. 10.

n	Δt_c (ns)	Δt_{nr} (ns)
1	0.7750	0.7520
2	0.7750	0.8
3	0.7750	0.7630
4	0.7750	0.7570
5	0.7750	0.8

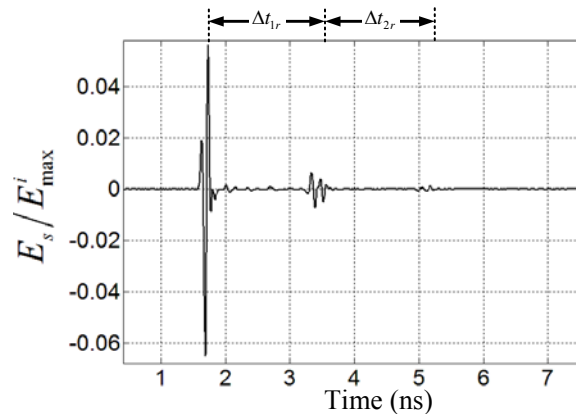


Fig. 11. TM_z back scattered field from a buried cylindrical PEC object for $r_a = 0.01$ m, $h_c = 0.06$ m, $wl = 2$ m, $x_c / r_a = 0.0$, $\epsilon_1 = 15 \epsilon_0$ F/m, $\mu_1 = \mu_0$ H/m, $\phi_i = \phi_s = 90^\circ$, $w_p = 0.1$ m, $h_p / w_p = 0.1$, and $\sigma_1 = 0.001 \text{ Sm}^{-1}$.

Table V: Comparison of timings for the case shown in Fig. 11.

n	Δt_c (ns)	Δt_{nr} (ns)
1	1.807	1.7030
2	1.807	1.7890

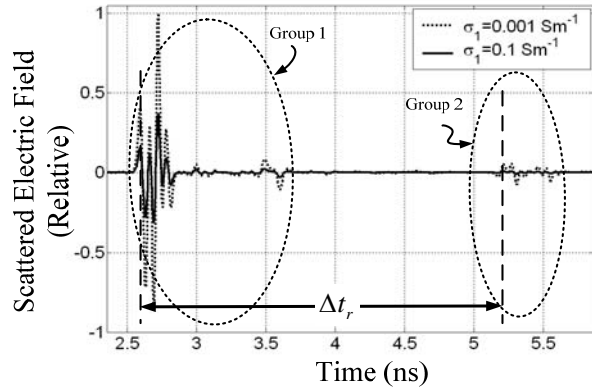


Fig. 12. TM_z back scattered field from a buried cylindrical PEC object for $r_a = 0.01$ m, $h_c = 0.1$ m, $wl = 2$ m, $x_c / r_a = 0.0$, $\epsilon_1 = 15 \epsilon_0$ F/m, $\mu_1 = \mu_0$ H/m, $\phi_i = \phi_s = 90^\circ$, $w_p = 0.1$ m, and $h_p/w_p = 0.1$.

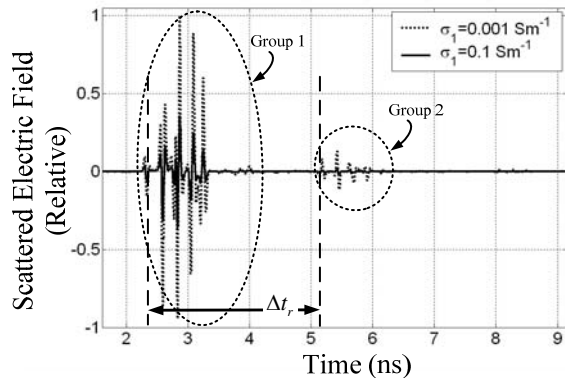


Fig. 13. TM_z back scattered field from a buried cylindrical PEC object for $r_a = 0.01$ m, $h_c = 0.1$ m, $wl = 2$ m, $x_c / r_a = 0.0$, $\epsilon_1 = 15 \epsilon_0$ F/m, $\mu_1 = \mu_0$ H/m, $\phi_i = \phi_s = 20^\circ$, $w_p = 0.1$ m, and $h_p/w_p = 0.1$.

IV. CONCLUSION

A two-dimensional model having a PEC cylindrical object buried in a lossy medium having a flat and slightly rough surface is developed for multipath analysis. A decomposition method solution is used to solve this scattering problem in our previous works. After getting the time domain

signals, the possible paths are identified by using the travelling time of reflected signals. Timing analysis shows that there are good agreements between the calculations and the relative results.

ACKNOWLEDGMENT

This research has been supported by Yildiz Technical University Scientific Research Projects Coordination Department. Project number: 2010-04-03-DOP01.

REFERENCES

- [1] J. D. Kanellopoulos and N. E. Buris, "Scattering from conducting cylinders embedded in a lossy medium," *International Journal of Electronics*, vol. 57, no. 3, pp. 391-401, 1984.
- [2] T. J. Cui, W. C. Chew, and W. Hong, "New approximate formulations for EM scattering by dielectric objects," *IEEE Transactions on Antennas and Propagation*, vol. 52, no. 3, pp. 684-692, 2004.
- [3] D. E. Lawrence and K. Sarabandi, "Electromagnetic scattering from a dielectric cylinder buried beneath a slightly rough surface," *IEEE Transactions on Antennas and Propagation*, vol. 50, no. 10, pp. 1368-1376, 2002.
- [4] Y. Altuncu, A. Yapar, and I. Akduman, "On the scattering of electromagnetic waves by bodies buried in a half-space with locally rough interface," *IEEE Trans. Geosci. Remote Sens.*, vol. 44, no. 6, pp. 1435-1443, 2006.
- [5] Q. A. Naqvi, A. A. Rizvi, and Z. Yaqoob, "Scattering of electromagnetic waves from a deeply buried circular cylinder," *Progress in Electromagnetics Research*, vol. 27, pp. 37-59, 2000.
- [6] Y. Altuncu, I. Akduman, and A. Yapar, "Detecting and locating dielectric objects buried under a rough interface," *IEEE Geoscience and Remote Sensing Letters*, vol. 4, no. 2, pp. 251-255, 2007.
- [7] C. C. Chiu and Y. W. Kiang, "Electromagnetic inverse scattering of a conducting cylinder buried in a lossy half-space," *IEEE Transactions on Antennas and Propagation*, vol. 40, pp. 1562-1565, 1992.
- [8] T. Dogaru and L. Carin, "Time-domain sensing of targets buried under a rough air-ground interface," *IEEE Transactions on Antennas and Propagation*, vol. 46, no. 3, pp. 360-372, 1998.
- [9] C. Huang, C. Chen, C. Chiu, and C. Li, "Reconstruction of the buried homogenous dielectric cylinder by FDTD and asynchronous particle swarm optimization," *Applied Computational Electromagnetics Society (ACES) Journal*, vol. 25, no. 8, pp. 672-681, August 2010.

- [10] F. Deek and M. El-Shenawee, "Microwave detection of cracks in buried pipes using the complex frequency technique," *Applied Computational Electromagnetics Society (ACES) Journal*, vol. 25, no. 10, pp. 894-902, Oct. 2010.
- [11] K. P. Prokopidis and T. D. Tsiboukis, "Modeling of ground-penetrating radar for detecting buried objects in dispersive soils," *Applied Computational Electromagnetics Society (ACES) Journal*, vol. 22, no. 2, pp. 287-294, July 2007.
- [12] C. H. Huang, C. C. Chiu, C. J. Lin, and Y. F. Chen, "Inverse scattering of inhomogeneous dielectric cylinders buried in a slab medium by TE wave illumination," *Applied Computational Electromagnetics Society (ACES) Journal*, vol. 22, no. 2, pp. 295-301, July 2007.
- [13] R. Araneo and S. Barmada, "Advanced image processing techniques for the discrimination of buried objects," *Applied Computational Electromagnetics Society (ACES) Journal*, vol. 26, no. 5, pp. 437-446, May 2011.
- [14] P. Falorni, L. Capineri, L. Masotti, and C. G. Windsor, "Analysis of time domain ultra-wide band radar signals reflected by buried objects," *Progress In Electromagnetics Research (PIERS)*, vol. 3, no. 5, pp. 662-665, 2007.
- [15] C. G. Windsor, L. Capineri, and P. Falorni, "The estimation of buried pipe diameters by generalized Hough transform of radar data," *Progress In Electromagnetics Research Symposium*, Hangzhou, China, pp. 345-349, August 2005.
- [16] S. Vitebskiy, K. Sturgess, and L. Carin, "Short-pulse plane-wave scattering from buried perfectly conducting bodies of revolution," *IEEE Transactions on Antennas and Propagation*, vol. 44, no. 2, pp. 143-151, February 1996.
- [17] S. Vitebskiy and L. Carin, "Moment-method modeling of short-pulse scattering from and the resonances of a wire buried inside a lossy, dispersive half-space," *IEEE Transactions on Antennas and Propagation*, vol. 43, no. 1, pp. 1303-1312, November 1995.
- [18] J. A. Fuller and J. R. Wait, "Electromagnetic pulse transmission in homogeneous dispersive rock," *IEEE Transactions on Antennas and Propagation*, vol. 20, no. 4, pp. 530-533, July 1972.
- [19] D. L. Moffai and R. J. Puskar, "A subsurface electromagnetic pulse radar," *Geophys.*, vol. 41, pp. 506-518, June 1976.
- [20] L. Peters Jr. and J. D. Young, *Applications of Subsurface Transient Radars*, in Eme Domain Measurements in Electromagnetics, New York Van Nostrand Reinhold, E. K. Miller, Ed., 1986.
- [21] G. S. Smith and W. R. Scott Jr., "A scale model for studying ground penetrating radars," *IEEE Trans. Geosci. Remote Sensing*, vol. 27, no. 4, pp. 358-363, 1989.
- [22] C. Liu and C. Shen, "Numerical simulation of subsurface radar for detecting buried pipes," *IEEE Trans. Geosci. Remote Sensing*, vol. 29, no. 5, pp. 795-798, Sept. 1991.
- [23] M. Jaureguy and P. Borderies, "Modelling and processing of ultra wide band scattering of buried targets," *EUREL International Conference on The Detection of Abandoned Land Mines: A Humanitarian Imperative Seeking a Technical Solution*, no. 431, p.119-123, 1996.
- [24] F. Sabath, *Ultra-Wideband Short-Pulse Electromagnetics 7*, Springer 2007.
- [25] kal and A. Kizilay, "A decomposition method for the electromagnetic scattering from a conductive object buried in a lossy medium," *Applied Computational Electromagnetics Society (ACES) Journal*, vol. 26, no. 4, pp. 340-347, 2011.
- [26] S. Makal and A. Kizilay, "Computation of the scattered fields from a dielectric object buried in a medium with a periodic surface by a decomposition method," *IET Microwaves, Antennas and Propagation*, vol. 5, no. 14, pp. 1703-1709, 2011.



Senem Makal Yucedag was born in Tunceli, Turkey, in 1983. She received B.Sc., M.Sc., and Ph.D. degrees in Electronics and Communications Engineering from Yildiz Technical University in 2005, 2007, and 2012, respectively. She is a senior researcher in the Center of Research for Advanced Technologies of Informatics and Information Security (TUBITAK). Her main research interests include electromagnetic wave theory, electromagnetic scattering, artificial neural networks, and radar target identification.



Ahmet Kizilay was born in Istanbul, Turkey, in 1969. He received B.Sc. degree in Electronics and Communications Engineering from Yildiz University in 1990, M.Sc. and Ph.D. degrees in Electrical Engineering from Michigan State University in 1994 and 2000, respectively. In July 2001, he joined the Department of Electronics and Communications Engineering at Yildiz Technical University, where he is currently working as Associate Professor. His main research interests include time domain electromagnetic scattering, electromagnetic wave theory, and fiber optics.